2896 *Inorg. Chem.* **1985**, *24*, 2896-2900

Contribution from the Molecular and Materials Research Division,
Lawrence Berkeley Laboratory, University of California, Berkeley, California 94720

Bridging of Thorium by Hydrogen Atoms of Methyltrihydroborate Groups. Crystal Structures of Bis[tetrakis(methyltrihydroborato)thorium(IV)] Etherate and Bis[tetrakis(methyltrihydroborato)thorium(IV) tetrahydrofuranate]

RON SHINOMOTO, JOHN G. BRENNAN, NORMAN M. EDELSTEIN,* and ALLAN ZALKIN*

Received September 7, 1984

Dimeric complexes of $Th(CH_3BH_3)_4$ with diethyl ether and tetrahydrofuran have been synthesized and the molecular structures determined by X-ray diffraction. $[Th(BH_3CH_3)_4]_2\cdot O(C_2H_5)_2$ is monoclinic, $P2_1/c$, $a = 20.163$ (5) Å, $b = 10.353$ (3) Å, $c = 14.583$ (3) Å, $\beta = 104.47$ (3)°, $Z = 4$, $d_x = 1.73$ g cm^{-3}; $R = 0.024$ ($F^2 > 2\sigma$). $[Th(BH_3CH_3)_4\cdot OC_4H_8]_2$ is monoclinic, $P2_1/n$, $a = 12.506$ (4) Å, $b = 11.533$ (4) Å, $c = 11.662$ (4) Å, $\beta = 99.06$ (2)°, $Z = 4$, $d_x = 1.68$ g cm^{-3}; $R = 0.019$ ($F^2 > 2\sigma$). The thorium atoms are bridged by two BH_3CH_3 ligands through one of the hydrogen atoms of each BH_3 group; the Th–Th distances are 4.445 (2) and 4.917 (2) Å for the ether and tetrahydrofuran complexes, respectively. The Th–B distances range from 2.48 to 2.63 Å for the terminal BH_3CH_3 groups and from 2.91 to 3.11 Å for the bridging BH_3CH_3 groups. The coordination number for Th is 13 for one of the two Th atoms in the ethyl ether complex and 14 for all the others. NMR and IR spectra suggest that the dimeric structure is not maintained in solution.

Introduction

Transition-metal and actinide complexes containing the tetrahydroborate ligand have been the subject of extensive studies because of their unusual chemical and physical properties. Structural studies have shown that the tetrahydroborate ligand can bond to the metal via monodentate, bidentate, or tridentate hydrogen bridges, and NMR solution studies have shown there is a very low barrier to bridge–terminal hydrogen exchange in the tetrahydroborate ligand.[1] The volatile compound $U(BH_4)_4$ is polymeric in the solid state due to tetrahydroborate groups that link U atoms by double hydrogen bridge bonds; each U atom is coordinated to four bidentate ligands plus two tridentate tetrahydroborate ligands, giving 14-coordination about the metal.[2] $Th(BH_4)_4$ and $Pa(BH_4)_4$ also exhibit this structure. However, $Np(BH_4)_4$ and $Pu(BH_4)_4$ are monomolecular in the solid state, being 12-coordinate with four tridentate tetrahydroborate groups coordinated to the metal atom,[3] with bonding that closely resembles that of $Zr(BH_4)_4$[4] and $Hf(BH_4)_4$.[5] The free energy for the structural transformation in the solid at 290 K from 14-coordinate $U(BH_4)_4$ to 12-coordinate $U(BH_4)_4$ has been estimated to be 2.6 kcal/mol from vapor pressure data.[6]

In the methyl, ethyl, and propyl ether complexes with $U(BH_4)_4$,[7] uranium atoms are bridged by tetrahydroborate groups through bidentate hydrogen bridges and are also coordinated to ether oxygen atoms and other tetrahydroborate groups through tridentate hydrogen bridges. The coordination numbers about the uranium atoms are 13 or 14.

The substitution of a methyl group for one of the H atoms on the tetrahydroborate ligand results in a 12-coordinate structure for $An(BH_3CH_3)_4$ (An = Th, U, Np).[8] We report the preparation and structure of two dimeric compounds, $[Th(BH_3CH_3)_4\cdot OC_4H_8]_2$ and $[Th(BH_3CH_3)_4]_2\cdot OEt_2$, which exhibit a different type of metal–metal bridging by methyltrihydroborate ligands.

Table I. Nuclear Magnetic Resonance Data[a]

$[Th(BH_3CH_3)_4]_2\cdot OEt_2$	$^1H^b$	+3.50 (24 H, q), +3.28 (4 H, q), +0.73 (6 H, t), +0.15 (24 H, q)
	$^{11}B^c$	−19.3 (q)
	$^{13}C\{^1H\}^b$	+68.6 (s), +13.1 (s), +7.56 (m)
$[Th(BH_3CH_3)_4\cdot THF]_2$	$^1H^b$	+3.67 (8 H, m), +3.44 (24 H, q), +0.99 (8 H, m), +0.36 (24 H, q)
	$^{11}B^c$	−19.3 (q)
	$^{13}C\{^1H\}^b$	+75.3 (s), +25.5 (s), +5.57 (m)

[a] All samples prepared in toluene-d_8 at 25 °C. [b] Shift in ppm from Me_4Si. Positive sign indicates a downfield shift. [c] Shift in ppm from boric acid. Positive sign indicates a downfield shift.

Table II. Infrared Spectroscopic Data

$[Th(BH_3CH_3)_4]_2\cdot OEt_2$	2950 m, 2160 m, 2060 s, 1310 s, 1250 s, 1090 s, 990 m, 910 m, 720 m
$[Th(BH_3CH_3)_4\cdot THF]_2$	2950 m, 2200 m, 2100 s, 1305 s, 1245 s, 1085 m, 1005 m, 970 m, 915 m, 845 s, 720 w, 670 w

Experimental Section

All preparations were carried out under an atmosphere of argon or under high vacuum. Diethyl ether and tetrahydrofuran were distilled from sodium benzophenone ketyl under argon. Hexane was dried over CaH_2 and distilled under argon. Melting points were determined in sealed argon-filled capillaries. $ThCl_4$ was dried with $SOCl_2$. $Th(BH_3CH_3)_4$[8] and $LiBH_3CH_3$[9] were prepared as described previously.

Infrared spectra were recorded on a Perkin-Elmer IR-283 spectrophotometer and calibrated with polystyrene film; Nujol and Fluorolube mulls were prepared in an argon-filled drybox with dry, degassed Nujol and Fluorolube. ^1H, ^{11}B, and ^{13}C NMR spectra were recorded on a JEOL FX 90Q 90-MHz FT spectrometer; samples were dissolved in toluene-d_8 inside an argon-filled drybox. NMR and IR data obtained at 25 °C are presented in Tables I and II, respectively.

Bis[tetrakis(methyltrihydroborato)thorium(IV)] Etherate. To 1.25 g (3.3 mmol) of $ThCl_4$ were added 0.49 g (13.7 mmol) of $LiBH_3CH_3$ and 20 mL of diethyl ether, and the mixture was stirred for 24 h under argon. The solvent was removed in vacuo to near dryness. The residue remaining was sublimed with pumping at room temperature into a 0 °C trap over a 12-h period. A yield of 0.52 g (37% yield) of an oil, which crystallized after several weeks into colorless crystals of $[Th(BH_3CH_3)_4]_2\cdot OEt_2$, was obtained. Mp: 92–93 °C. A consistent elemental analysis was not obtained.

Bis[tetrakis(methyltrihydroborato)thorium(IV) tetrahydrofuranate]. To 0.27 g (0.78 mmol) of $Th(BH_3CH_3)_4$ dissolved in about 20 mL of hexane was added 0.063 mL (0.78 mmol) of THF with stirring. The mixture was stirred for several hours and pumped dry and the residue sublimed at 100 °C in vacuo. A yield of 0.25 g (85% yield) of colorless $[Th(BH_3CH_3)_4\cdot THF]_2$ was recovered; mp 112–114 °C. Anal. Calcd for $C_{16}H_{64}B_8O_2Th_2$: C, 22.90; H, 7.69. Found: C, 23.06; H, 7.77.

Colorless crystals were sealed inside quartz capillaries in an argon-filled drybox. X-ray diffraction intensities were obtained by using a

---

(1) Marks, T. J.; Kolb, J. R. *Chem. Rev.* **1977**, *77*, 263.

(2) (a) Bernstein, E. R.; Keiderling, T. A.; Lippard, S. J.; Mayerle, J. J. *J. Am. Chem. Soc.* **1972**, *94*, 2522. (b) Bernstein, E. R.; Hamilton, W. C.; Keiderling, T. A.; LaPlaca, S. J.; Lippard, S. J.; Mayerle, J. J. *Inorg. Chem.* **1972**, *11*, 3009.

(3) Banks, R. H.; Edelstein, N. M.; Spencer, B.; Templeton, D. H.; Zalkin, A. *J. Am. Chem. Soc.* **1980**, *102*, 620.

(4) Bird, P. H.; Churchill, M. R. *J. Chem. Soc., Chem. Commun.* **1967**, 403.

(5) Keiderling, T. A. Ph.D. Thesis, Princeton University, 1974.

(6) Banks, R. H.; Edelstein, N. M. *ACS Symp. Ser.* **1980**, *No.* 131, 331.

(7) (a) Rietz, R. R.; Zalkin, A.; Templeton, D. H.; Edelstein, N. M.; Templeton, L. K. *Inorg. Chem.* **1978**, *17*, 653. (b) Zalkin, A.; Rietz, R. R.; Templeton, D. H.; Edelstein, N. M. *Inorg. Chem.* **1978**, *17*, 661.

(8) Shinomoto, R.; Gamp, E.; Edelstein, N. M.; Templeton, D. H.; Zalkin, A. *Inorg. Chem.* **1983**, *22*, 2351.

(9) Wartik, T.; Schlesinger, H. I. *J. Am. Chem. Soc.* **1953**, *75*, 835.

Table III. X-ray, Crystal, and Least-Squares Refinement Parameters

	$[Th(BH_3CH_3)_4]_2 \cdot O(C_2H_5)_2$	$[Th(BH_3CH_3)_4 \cdot OC_4H_8]_2$
	A. Crystal Parameters[a]	
cryst syst	monoclinic	monoclinic
space group	$P2_1/c$	$P2_1/n$
a, Å	20.163 (5)	12.506 (4)
b, Å	10.353 (3)	11.533 (4)
c, Å	14.583 (3)	11.662 (4)
β, deg	104.47 (3)	99.06 (2)
V, Å^3	2947.6	1661.1
T, °C	23	23
Z	4	2
mol wt	769.16	839.26
d_{calcd}, g/cm^3	1.73	1.68
	B. Intensity Data	
radiation	Mo Kα[g]	Mo Kα[g]
2θ range, deg	4–45	4–50
scan type	θ(cryst)–2θ(counter)	θ(cryst)–2θ(counter)
scan speed, deg/min	variable 2–8	variable 2–8
scan range	$1.4 + 0.693 \tan \theta$	$1.2 + 0.693 \tan \theta$
reflcns measd	$\pm h,+k,\pm l$ (2 forms)	$\pm h,+k,\pm l$ (2 forms)
no. of reflcns collcd	9095	5865
no. of unique reflcns	4058	2940
cryst size, mm	0.10 × 0.12 × 0.15	0.15 × 0.18 × 0.22
abs coeff cm^{-1}	104	93
abs cor range	2.4–3.6	3.3–4.7
cryst decay cor	1.00–1.20	1.00–1.04
extinction cor[b]	0.21×10^{-6}	0.14×10^{-6}
	C. Least-Squares Refinement	
no. of data used ($F^2 > 2\sigma$)	2265[c]	1923
p[d]	0.02	0.025
R ($F^2 > 2\sigma$)[e]	0.024	0.019
R_w	0.021	0.020
σ_1[f]	1.09	0.99
max shift/esd (non-hydrogen atoms)	0.04	0.09

[a] Cell dimensions based on a least-squares fit to the setting angles of unresolved Mo Kα peaks of 28 reflections with $2\theta = 5–47°$ for the etherate and 42 reflections with $2\theta = 19–34°$ for the tetrahydrofuran complex. [b] The empirical extinction correction has the form $F_{cor} = F_{obsd}(1 + kI_{obsd})$, where F is the structure factor, I is the observed intensity, and k is the extinction factor. [c] Because of some large discrepancies in the low-angle data, all 45 data below $(\sin \theta)/\lambda < 0.14$ were deleted. [d] See ref 11. [e] $R = \sum||F_o| - |F_c||/\sum|F_o|$. $R_w = [\sum w(\Delta F)^2/\sum wF_o^2]^{1/2}$. [f] σ_1 = standard deviation of an observation of unit weight = $[\sum w(\Delta F)^2)/(n - v)]^{1/2}$, where n = number of reflections and v = number of parameters. [g] λ(Kα) = 0.71073 Å, graphite monochromated.

modified Picker FACS-I diffractometer. The details of the analysis are given in Table III. The intensities were corrected for absorption by an analytical method.[10] Standard reflections were measured after every 250 data, and the data were adjusted accordingly.

Thorium atom positions were deduced from three-dimensional Patterson functions. The structure factors were assigned phases on the basis of the thorium atoms, and electron density calculations were used to find the positions of the oxygen, boron, and carbon atoms. The positional and anisotropic thermal parameters of all the non-hydrogen atoms were refined to convergence by full-matrix least squares.[11] Most of the hydrogen atoms were located in the difference maps, and for those that were not found, their positions could be estimated. In the THF complex all of the hydrogen atoms were included in the least-squares refinements with isotropic thermal parameters. Some of the thermal parameters, in particular for the hydrogen atoms on carbon, refined to unrealistic values; therefore, for these hydrogen atoms two isotropic thermal parameters were used, one for the methyl hydrogen atoms and one for the hydrogen atoms of the THF ligand. In the ether complex many of the hydrogen parameters would not refine to values that made chemical sense; therefore, only the bridging hydrogen atoms (hydrogens on B(1) and B(8)) were allowed to refine in an unrestrained manner, and the remaining hydrogen atoms were included with distance restraints.[12] The distance restraints used were as follows: C–H, 1.00 ± 0.04 Å; B–H, 1.16 ± 0.04 Å; H–H (methyl and methylene), 1.62 ± 0.05 Å; H–H (BH_3), 1.875 ± 0.05 Å; H(methyl or methylene)–C(next neighbor), 2.01 ± 0.06 Å; H(methyl)–B(next neighbor), 2.13 ± 0.06 Å; H(BH_3)–C(next neighbor), 2.36 ± 0.06 Å. These restraints impose tetrahedral symmetry on the BH_3 and CH_3 groups and 3-fold symmetry along B–C bonds but allow the triad of hydrogen atoms to rotate about the B–C bond. Five isotropic thermal parameters were used on the restrained atoms, one for the BH_3-group hydrogens, one for the methyl hydrogens of the BH_3CH_3 groups, one for the methyl hydrogens of the ether, and one for the methylene hydrogens of the ether. Final positional parameters are listed in Table IV. Lists of thermal parameters, restraints, and structure factors are given in the supplementary material.

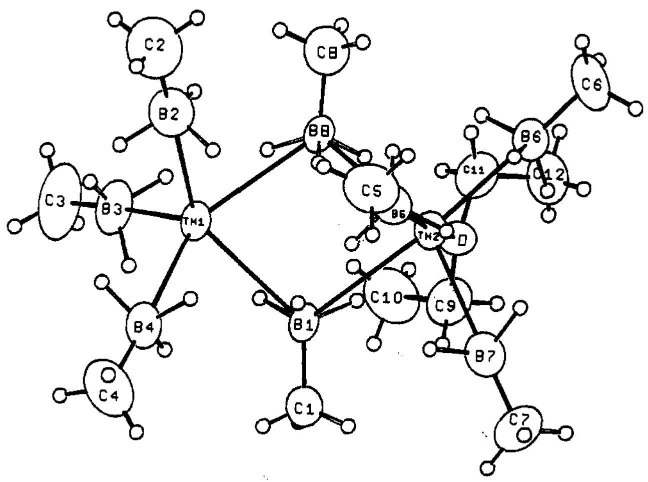

Figure 1. ORTEP drawing of the $[Th(BH_3CH_3)_4]_2 \cdot O(C_2H_5)_2$ molecule.

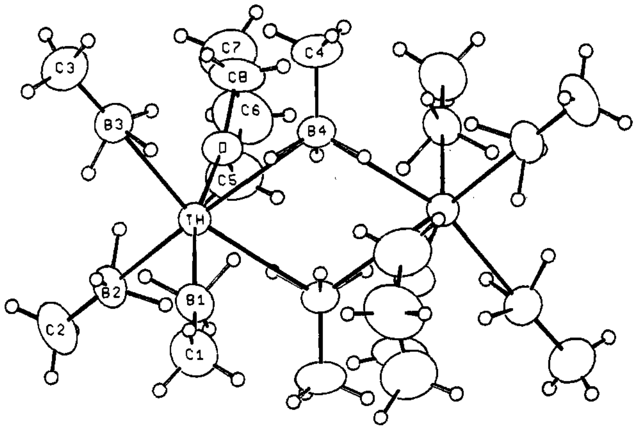

Figure 2. ORTEP drawing of the $[Th(BH_3CH_3)_4 \cdot OC_4H_8]_2$ molecule.

Results and Discussion

Drawings of the structures are shown in Figures 1 and 2, and selected distances and angles are given in Tables V and VI. In both complexes two thorium atoms are bridged by two methyltrihydroborate groups to form dimers, and each Th atom is bonded to three additional BH_3CH_3 groups. In the diethyl ether complex only one of the two thorium atoms is coordinated to an ether ligand whereas in the tetrahydrofuran complex each thorium atom is coordinated to a THF ligand.

The nonbridging BH_3CH_3 groups bond in the same fashion as the methyltrihydroborate groups found in $An(BH_3CH_3)_4$ (An = Th, U, Np), in which the metal atom is connected to the boron atom by a tridentate hydrogen bridge.[2] The nonbridged Th–B distances range from 2.48 to 2.63 Å, averaging 2.58 ± 0.05 Å, and are comparable to the average distance of 2.56 ± 0.05 Å in $Th(BH_3CH_3)_4$.[8]

---

(10) Templeton, L. K.; Templeton, D. H. "Abstracts of Papers" American Crystallographic Proceedings, Series 2, Vol. 2, 1973; p 143.

(11) The function minimized in the least-squares refinement was $\sum w(|F_o| - |F_c|)^2$, where $w = [\sigma(F)]^{-2}$ is derived from $\sigma(F^2) = [S^2 + (pF^2)^2]^{1/2}$, where S^2 is the variance due to counting and $p = 0.02$.

(12) Waser, J. *Acta Crystallogr.* **1963**, *16*, 1091.

Table IV. Positional Parameters

a. $[Th(BH_3CH_3)_4]_2{\cdot}O(C_2H_5)_2$

atom	*x*	*y*	*z*	atom	*x*	*y*	*z*
Th(1)	0.37554 (1)	0.01437 (5)	0.35320 (2)	C(5)	0.1614 (6)	−0.0177 (12)	0.4910 (7)
Th(2)	0.15492 (2)	0.01709 (4)	0.20180 (2)	C(6)	0.0067 (6)	−0.2581 (12)	0.1128 (9)
O	0.16138 (27)	0.0069 (6)	0.0268 (4)	C(7)	0.0617 (6)	0.3756 (11)	0.1650 (8)
B(1)	0.2834 (7)	0.1837 (12)	0.2188 (11)	C(8)	0.2617 (7)	−0.3040 (11)	0.2539 (10)
B(2)	0.3798 (8)	−0.1652 (14)	0.4786 (10)	C(9)	0.1787 (7)	0.1138 (12)	−0.0276 (9)
B(3)	0.4768 (6)	−0.0231 (15)	0.2894 (8)	C(10)	0.2448 (7)	0.0987 (13)	−0.0480 (10)
B(4)	0.4067 (7)	0.2172 (13)	0.4560 (11)	C(11)	0.1531 (7)	−0.1153 (11)	−0.0243 (9)
B(5)	0.1612 (6)	−0.0051 (12)	0.3830 (7)	C(12)	0.0936 (7)	−0.1183 (12)	−0.1033 (9)
B(6)	0.0623 (6)	−0.1530 (12)	0.1446 (9)	H(1)	0.270 (4)	0.156 (7)	0.299 (6)
B(7)	0.0972 (7)	0.2414 (12)	0.1756 (8)	H(2)	0.256 (5)	0.137 (8)	0.160 (7)
B(8)	0.2708 (8)	−0.1588 (12)	0.2327 (12)	H(3)	0.329 (4)	0.129 (7)	0.210 (5)
C(1)	0.2837 (6)	0.3333 (10)	0.2036 (9)	H(22)	0.236 (3)	−0.117 (5)	0.159 (4)
C(2)	0.3841 (9)	−0.2708 (15)	0.5567 (12)	H(23)	0.311 (4)	−0.130 (7)	0.228 (5)
C(3)	0.5413 (6)	−0.0408 (18)	0.2548 (10)	H(24)	0.264 (4)	−0.099 (7)	0.289 (5)
C(4)	0.4288 (8)	0.3390 (13)	0.5231 (11)				

b. $[Th(BH_3CH_3)_4{\cdot}OC_4H_8]_2$

atom	*x*	*y*	*z*	atom	*x*	*y*	*z*
Th	0.09245 (2)	0.12550 (2)	0.15507 (2)	H(10)	−0.066 (5)	0.156 (6)	0.022 (6)
O	0.0079 (4)	−0.0323 (4)	0.2627 (4)	H(11)	−0.136 (4)	0.061 (4)	−0.100 (4)
B(1)	0.1763 (7)	0.2500 (8)	0.0046 (7)	H(12)	−0.079 (4)	0.004 (5)	0.041 (5)
B(2)	0.2694 (8)	0.0924 (9)	0.3036 (9)	H(13)	0.244 (8)	0.270 (9)	−0.154 (9)
B(3)	−0.0016 (8)	0.2875 (9)	0.2631 (9)	H(14)	0.298 (9)	0.360 (10)	−0.065 (9)
B(4)	−0.1289 (6)	0.0817 (7)	−0.0012 (7)	H(15)	0.198 (9)	0.411 (10)	−0.115 (10)
C(1)	0.2248 (9)	0.3305 (9)	−0.0850 (9)	H(16)	0.393 (9)	−0.012 (10)	0.423 (9)
C(2)	0.3773 (7)	0.0801 (8)	0.3930 (9)	H(17)	0.379 (8)	0.110 (10)	0.470 (9)
C(3)	−0.0512 (10)	0.3915 (10)	0.3227 (11)	H(18)	0.443 (8)	0.065 (10)	0.382 (10)
C(4)	−0.2441 (7)	0.1121 (11)	0.0320 (10)	H(19)	−0.123 (9)	0.414 (11)	0.303 (12)
C(5)	0.0596 (9)	−0.1433 (8)	0.3033 (9)	H(20)	−0.055 (12)	0.430 (11)	0.268 (10)
C(6)	−0.0147 (11)	−0.2030 (11)	0.3692 (12)	H(21)	−0.076 (11)	0.382 (14)	0.377 (10)
C(7)	−0.1038 (11)	−0.1200 (14)	0.3804 (10)	H(22)	−0.275 (10)	0.054 (10)	0.028 (12)
C(8)	−0.1023 (7)	−0.0385 (10)	0.2881 (10)	H(23)	−0.294 (9)	0.164 (9)	−0.014 (9)
H(1)	0.179 (4)	0.281 (5)	0.091 (5)	H(24)	−0.243 (8)	0.103 (11)	0.113 (9)
H(2)	0.216 (6)	0.152 (6)	0.028 (6)	H(25)	0.129 (8)	−0.122 (10)	0.342 (9)
H(3)	0.098 (6)	0.224 (7)	−0.015 (6)	H(26)	0.060 (9)	−0.177 (9)	0.237 (9)
H(4)	0.248 (8)	0.144 (10)	0.286 (11)	H(27)	0.015 (9)	−0.223 (11)	0.432 (10)
H(5)	0.249 (3)	0.053 (4)	0.225 (4)	H(28)	−0.039 (10)	−0.269 (10)	0.348 (10)
H(6)	0.185 (5)	0.078 (6)	0.336 (5)	H(29)	−0.117 (9)	−0.094 (10)	0.446 (9)
H(7)	0.000 (6)	0.294 (7)	0.158 (7)	H(30)	−0.177 (8)	−0.163 (9)	0.379 (9)
H(8)	0.077 (7)	0.282 (7)	0.269 (7)	H(31)	−0.144 (9)	−0.051 (11)	0.240 (10)
H(9)	−0.025 (9)	0.197 (10)	0.251 (10)	H(32)	−0.126 (9)	0.042 (9)	0.286 (10)

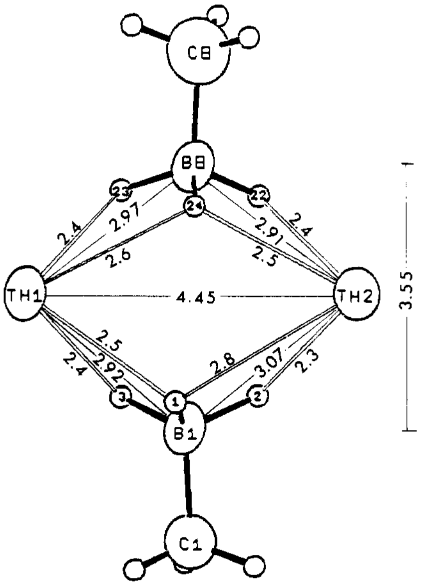

Figure 3. Bridging scheme in $[Th(BH_3CH_3)_4]_2{\cdot}O(C_2H_5)_2$.

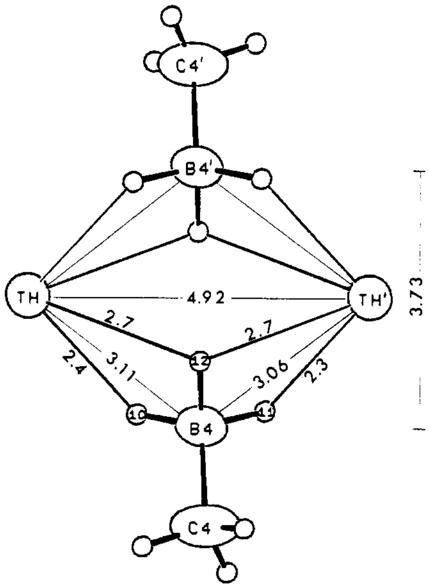

Figure 4. Bridging scheme in $[Th(BH_3CH_3)_4{\cdot}OC_4H_8]_2$.

The geometry of the double bridge is illustrated in Figures 3 and 4. The three hydrogen atoms of the BH_3 group connect the Th and B atoms. The Th atoms have sole contact with two hydrogen atoms and share two other hydrogen atoms for a total of four hydrogen contacts. For the THF complex the average Th–H(nonbridging) and Th–H(bridging) distances are 2.27 (6) and 2.72 (1) Å, respectively; in the ether complex the two comparable average distances are 2.38 (8) and 2.60 (13) Å.

The geometries of the bridging portion of the two complexes are different (Figures 3 and 4). In the ethyl ether complex (Figure 3) the bridging hydrogens H(1) and H(24) are cis to each other, and the four atoms Th(1), B(1), Th(2), and B(8) are not in a

Table V. Selected Distances (Å)

	$[Th(BH_3CH_3)_4]_2 \cdot O(C_2H_5)_2$			$[Th(BH_3CH_3)_4 \cdot OC_4H_8]_2$	
Th(1)–B(2)	2.60 (2)	Th(2)–B(5)	2.62 (1)	Th–B(1)	2.611 (8)
Th(1)–B(3)	2.48 (2)	Th(2)–B(6)	2.55 (2)	Th–B(2)	2.615 (10)
Th(1)–B(4)	2.57 (2)	Th(2)–B(7)	2.58 (2)	Th–B(3)	2.632 (9)
Th(1)–B(1)	2.92 (2)	Th(2)–B(8)	2.91 (2)	Th–B(4)	3.107 (8)
Th(1)–B(8)	2.98 (2)	Th(2)–B(1)	3.07 (2)	Th–B(4)[a]	3.065 (8)
		Th(2)–O	2.59 (1)	Th–O	2.535 (4)
B(1)–C(1)	1.57 (2)	B(5)–C(5)	1.58 (2)	B(1)–C(1)	1.59 (1)
B(2)–C(2)	1.57 (2)	B(6)–(6)	1.55 (2)	B(2)–C(2)	1.58 (2)
B(3)–C(3)	1.52 (2)	B(7)–C(7)	1.55 (2)	B(3)–C(3)	1.56 (2)
B(4)–C(4)	1.59 (2)	B(8)–C(8)	1.55 (2)	B(4)–C(4)	1.59 (1)
		O–C(9)	1.45 (2)	O–C(5)	1.48 (1)
		O–C(11)	1.46 (2)	O–C(8)	1.46 (2)
		C(9)–C(10)	1.45 (2)	C(5)–C(6)	1.47 (2)
		C(11)–C(12)	1.44 (2)	C(6)–C(7)	1.49 (2)
				C(7)–C(8)	1.43 (2)
Th(1)–Th(2)	4.445 (2)			Th–Th[a]	4.917 (2)
B(1)–B(8)	3.565 (6)			B(4)–B(4)[a]	3.73 (2)
				av Th–H(unbridged)	2.27 ± 0.06
				av Th–H(bridged)	2.73 ± 0.01
				av B–H	1.09 ± 0.13
				av C–H(BH_3CH_3)	0.94 ± 0.12
				av C–H(THF)	0.90 ± 0.10

[a] Atom at $-x$, $-y$, $-z$.

Table VI. Selected Angles (deg)

	$[Th(BH_3CH_3)_4]_2 \cdot O(C_2H_5)_2$		
B(1)–Th(1)–B(8)	74.2 (4)	O–Th(2)–B(6)	82.1 (3)
B(1)–Th(1)–B(2)	143.7 (5)	O–Th(2)–B(7)	91.3 (3)
B(1)–Th(1)–B(3)	106.7 (4)	B(1)–Th(2)–B(5)	98.1 (4)
B(1)–Th(1)–B(4)	85.6 (5)	B(1)–Th(2)–B(6)	161.5 (4)
B(8)–Th(1)–B(2)	83.0 (5)	B(1)–Th(2)–B(7)	81.2 (4)
B(8)–Th(1)–B(3)	103.3 (4)	B(8)–Th(2)–B(5)	87.4 (4)
B(8)–Th(1)–B(4)	150.5 (4)	B(8)–Th(2)–B(6)	96.5 (4)
B(2)–Th(1)–B(3)	105.5 (5)	B(8)–Th(2)–B(7)	154.3 (4)
B(2)–Th(1)–B(4)	102.4 (5)	B(5)–Th(2)–B(6)	96.7 (4)
B(3)–Th(1)–B(4)	104.1 (5)	B(5)–Th(2)–B(7)	97.7 (4)
Th(1)–B(1)–C(1)	131.6 (9)	B(6)–Th(2)–B(7)	107.8 (5)
Th(1)–B(8)–C(8)	124.4 (9)	Th(2)–B(1)–C(1)	125.3 (8)
Th(1)–B(2)–C(2)	178.1 (4)	Th(2)–B(8)–C(8)	120.4 (9)
Th(1)–B(3)–C(3)	176.6 (10)	Th(2)–B(5)–C(5)	177.4 (9)
Th(1)–B(4)–C(4)	177.3 (10)	Th(2)–B(6)–C(6)	178.4 (9)
B(1)–Th(2)–B(8)	73.2 (4)	Th(2)–B(7)–C(7)	177.0 (8)
O–Th(2)–B(1)	81.6 (3)	Th(2)–O–C(9)	125.8 (6)
O–Th(2)–B(8)	83.8 (4)	Th(2)–O–C(11)	120.8 (6)
O–Th(2)–B(5)	170.8 (3)	C(9)–O–C(11)	113.2 (7)
	$[Th(BH_3CH_3)_4 \cdot OC_4H_8]_2$		
B(4)–Th–B(4)[a]	74.4 (2)	B(2)–Th–B(4)[a]	94.9 (3)
O–Th–B(4)	76.8 (2)	B(3)–Th–B(4)	88.4 (3)
O–Th–B(4)[a]	80.9 (2)	B(3)–Th–B(4)[a]	162.3 (3)
O–Th–B(1)	166.1 (3)	Th–B(1)–C(1)	177.5 (7)
O–Th–B(2)	86.7 (3)	Th–B(2)–C(2)	176.8 (7)
O–Th–B(3)	91.1 (3)	Th–B(3)–C(3)	175.0 (8)
B(1)–Th–B(2)	97.9 (3)	Th–B(4)–C(4)	125.4 (6)
B(1)–Th–B(3)	100.9 (4)	Th[a]–B(4)–C(4)	122.6 (6)
B(1)–Th–B(4)	96.3 (3)	Th–B(4)–Th[a]	105.6 (2)
B(1)–Th–B(4)[a]	85.6 (3)	Th–O–C(5)	125.8 (5)
B(2)–Th–B(3)	100.5 (4)	Th–O–C(8)	128.2 (5)
B(2)–Th–B(4)	161.4 (3)	C(5)–O–C(8)	105.8 (7)

[a] Atom at $-x$, $-y$, $-z$.

Table VII. ^1H NMR Data for $U(BH_3CH_3)_4$ + THF at −80 °C[a,b]

peak	shift	assignt
1	265.05	BH_3, $U(BH_3CH_3)_4 \cdot 2THF$
2	220.40	BH_3, $U(BH_3CH_3)_4$
3	143.17	BH_3, $U(BH_3CH_3)_4 \cdot THF$
4	65.39	THF, $U(BH_3CH_3)_4 \cdot THF$
5	34.14	THF, $U(BH_3CH_3)_4 \cdot THF$
6	30.91	CH_3, $U(BH_3CH_3)_4 \cdot 2THF$
7	22.86	CH_3, $U(BH_3CH_3)_4$
8	7.89	CH_3, $U(BH_3CH_3)_4 \cdot THF$
9	−24.79	THF, $U(BH_3CH_3)_4 \cdot 2THF$
10	−50.91	THF, $U(BH_3CH_3)_4 \cdot 2THF$

[a] In toluene-d_8. [b] Shifts in ppm from Me_4Si. Positive sign indicates downfield shift.

plane. In the tetrahydrofuran complex (Figure 4) the hydrogen atoms H(12) and H(12)′ are trans to each other across a center of symmetry, and the four atoms Th, B(4), Th′, and B(4)′ define an exact plane. In the ethyl ether structure, the coordination numbers are 13 and 14 for Th(1) and Th(2), respectively, whereas in the tetrahydrofuran complex the coordination number of both Th atoms is 14.

The steric properties of the base affect the bonding mode of the methyltrihydroborate ligand. Because of its bulkier nature, there is only space for diethyl ether to coordinate to one of the Th atoms while the less demanding THF can coordinate to both Th atoms. In previous studies,[7] similar results were found for the $U(BH_4)_4$ ether complexes, where the methyl and ethyl ether complexes are symmetric polymeric species with 14-coordinated U atoms, while the *n*-propyl ether complex is an asymmetric dimeric species, with one 14-coordinate and one 13-coordinate uranium atom. The larger *n*-propyl ether group is coordinated to only one of the two U atoms while the less bulky methyl and ethyl ether groups are coordinated to all U atoms.

The methyltrihydroborate ligand serves in a unique bridging capacity since it cannot form bidentate hydrogen bridges between adjacent metal atoms like the tetrahydroborates, due to the presence of the methyl group. Holah et al. reported a similar type of bridging for the tetrahydroborate complex $Co_2(BH_4)_2(Ph_2P(CH_2)_5PPh_2)_2 \cdot {}^1/_2C_6H_6$.[13]

The IR bands are similar to those of the tridentate $Th(BH_3CH_3)_4$ molecule with the addition of bands from the ether or THF molecules. There is no evidence for a bridging structure in the IR spectra of the Nujol mulls, in contrast to the report by Holah et al. for their Co tetrahydroborate complex.

Both diamagnetic Th dimers have been studied by $^{11}B\{^1H\}$, $^1H\{^{11}B\}$, and $^{13}C\{^1H\}$ NMR spectroscopy down to −96 °C in toluene-d_8, and there is no evidence for magnetically inequivalent methyltrihydroborate ligands. This can result from a solution structure different from the solid-state structure and/or a site-exchange process rapid on the ^1H NMR time scale. There is evidence for both. In order to increase the range of NMR-observable exchange rates, we have carried out solution studies using

---

(13) Holah, D. G.; Hughes, A. N.; Maciaszek, S.; Magnuson, V. R. *J. Chem. Soc., Chem. Commun.* **1983**, 1308.

the paramagnetic $U(BH_3CH_3)_4$. While the analogous uranium dimers have not yet been reproducibly isolated, a 1:1 mixture of $U(BH_3CH_3)_4$ and THF can be probed by NMR to determine what possible species exist in solution. The low-temperature ^1H NMR spectrum of $U(BH_3CH_3)_4$ and 1 equiv of THF in toluene-d_8 is reported in Table VII. At low temperatures (<−30 °C), peaks with chemical shifts identical with those of authentic compounds can be observed for $U(BH_3CH_3)_4$ and $U(BH_3CH_3)_4{\cdot}2THF$.[14] In addition, a third species is present, having integrated intensities 12:12:4:4—$U(BH_3CH_3)_4{\cdot}THF$. There is no evidence (down to −96 °C) for inequivalent methyltrihydroborate sites, and so $U(BH_3CH_3)_4{\cdot}THF$ is probably monomeric in solution. K_{eq} (by integration) for the reaction

$$U(BH_3CH_3)_4 + U(BH_3CH_3)_4{\cdot}2THF \rightleftarrows 2U(BH_3CH_3)_4{\cdot}THF$$

is ~20 at −80 °C. This indicates that the dimers isolated in the solid state are likely to have a more complex solution state.

Upon mixing equimolar amounts of $U(BH_3CH_3)_4$ and $Th(BH_3CH_3)_4$ in toluene-d_8 and recording the ^1H variable-temperature NMR spectra, we observe well-resolved peaks for both the Th and U compounds at low temperatures. As the solution temperature is raised, the BH_3 peaks broaden and the CH_3 peaks coalesce, becoming one time-averaged signal. The observed rate is concentration dependent. If under identical conditions Zr is substituted for Th (decreasing the ionic radius by 0.15 Å), no exchange is observed up to 80 °C. The resultant chemical shift of the Th/U exchange process is the weighted average of the individual species (within experimental error). These observations are consistent with an associative BH_3CH_3 exchange process and suggest that rapid methyltrihydroborate site exchange via a transient dimeric species is a plausible explanation for the lack of inequivalent sites observed in the NMR spectra of the diamagnetic thorium dimers.

Acknowledgment. This work was supported by the Director, Office of Energy Research, Office of Basic Energy Sciences, Chemical Sciences Division of the U.S. Department of Energy, under Contract No. DE-AC03-76SF00098.

Registry No. $[Th(BH_3CH_3)_4]_2{\cdot}OEt_2$, 97295-99-3; $[Th(BH_3CH_3)_4{\cdot}THF]_2$, 97296-00-9.

Supplementary Material Available: Lists of anisotropic thermal parameters, distance restraints on H atoms, hydrogen positional and thermal parameters, H atom distances, and observed structure factors (33 pages). Ordering information is given on any current masthead page.

---

[14] Shinomoto, R., unpublished results.

Contribution from the Department of Chemistry, Washington State University, Pullman Washington 99164,
Istituto di Chimica delle Macromolecole del CNR, Milano, Italy,
Istituto di Chimica Generale e Inorganica, Università di Modena, Modena, Italy,
and Istituto Chimico, Facoltà di Ingegneria, Università di Bologna, Bologna, Italy

Crystal Structure and Spectroscopic, Magnetic, and Electrical Properties of a Copper(II) Dimer, Melaminium Hexachlorodicuprate(II), Exhibiting a New Stacking Interaction

A. COLOMBO,[1a] L. MENABUE,[1b] A. MOTORI,[1c] G. C. PELLACANI,*[1b] W. PORZIO,[1a] F. SANDROLINI,[1c] and R. D. WILLETT[1d]

Received October 8, 1984

The $(C_3N_6H_8)Cu_2Cl_6$ compound ($C_3N_6H_8$ = melaminium dication, hereafter abbreviated as melH$_2$) has been synthesized and its crystal structure determined. A number of its physical properties were examined, including its electronic and vibrational spectra, as well as magnetic and electrical behavior. The crystals are monoclinic, space group $P2_1/c$, with a = 6.6600 (1) Å, b = 10.0598 (2) Å, c = 19.2691 (12) Å, β = 96.011 (3)°, Z = 4, d_{calcd} = 2.42 g·cm^{-3}, and d_{measd} = 2.45 g·cm^{-3}. The structure, solved by direct methods and refined by least-squares calculations to R = 3.9%, consists of melaminium dications and $Cu_2Cl_6^{2-}$ dimers stacked to form infinite chains in a manner not previously observed. The coordination of the copper atoms may be described as distorted square pyramidal. Electronic and vibrational results are discussed on the basis of the crystal structure. The compound exhibits predominantly antiferromagnetic exchange interactions. An intradimer singlet–triplet energy splitting of $\Delta E/k$ = 54 K is deduced, with weaker ferromagnetic coupling between dimers. A comparison with the magnetic behavior of other $Cu_2Cl_6^{2-}$ dimers is given. Electrical conductivity measurements classify the compound as an insulating material.

Introduction

The copper(II) ion plays a significant role in transition-metal chemistry, impacting on such areas as catalysis, bioinorganic chemistry, magnetic interactions, electrical conductors in solids, etc. The stereochemistry of the copper(II) ion is certainly the most rich among the ionic transition-metal complexes. Even with the simple halide ligands, a nearly continuous range of stereochemistries is obtained. This "softness" of the copper(II) coordination sphere has allowed the systematic exploration of the magnetostructural correlations covering a wide range of structural parameters. These correlations have been successfully applied to the synthesis of a large number of low-dimensional magnetic systems. It appears that many aspects of these variations in coordination geometry can be largely rationalized on the basis of a balance between crystal field stabilization and electrostatic effects. In the case of A_nCuX_{2+n} type systems, where A is an organic ammonium cation, the electrostatic effects are modulated by the precise nature of the organic groups. This has been noted in a recent review of the structures of $ACuCl_3$ salts.[2] Three classes of structures were observed: (1) isolated $Cu_2Cl_6^{2-}$ dimers; (2) $Cu_2Cl_6^{2-}$ dimers stacked to form chains; (3) uniform $(CuCl_3)_n^{n-}$ chains. The first class occurs with large cations with little or no hydrogen-bonding capabilities. The last two classes occur with small and/or strong hydrogen-bonding cations. For class 2, a simple graphic representation of the packing of the $Cu_nX_{2n+2}^{2-}$ polymers has been given, and a nomenclature has been developed.[3] A large number of permutations of stacking patterns for the

---

[1] (a) Istituto di Chimica delle Macromolecule del CNR. (b) Università di Modena. (c) Università di Bologna. (d) Washington State University.

[2] Willett, R. D.; Geiser, U. *Croat. Chem. Acta*, in press, and references cited therein.

[3] (a) Willett, R. D.; Geiser, U. XIII International Union of Crystallography Congress, Hamburg, 1984. (b) Geiser, U.; Willett, R. D.; Lind, M.; Emerson, K., to be submitted for publication in *Inorg. Chem.*